Multiphase modelling of the macrosegregation in ingot castings

M. Wu[1,2*], J. Li[1,2], A. Kharicha[2], A. Ludwig[2]

[1] Christian Doppler Laboratory for Advanced Process Simulation of Solidification and Melting,
[2] Chair of Simulation and Modelling of Metallurgical Processes, Univ. of Leoben, Austria
[*] Corresponding author, Franz-Josef-Str. 18, A-8700 Leoben, Austria, email: menghuai.wu@unileoben.ac.at

Abstract. A brief overview of the state-of-the-art modelling approaches for the macrosegregation in ingot castings is presented, with the emphasis on the recent activities of the multiphase model development being taken up by the current authors at the University of Leoben. A three-phase model for the mixed columnar-equiaxed solidification was recently proposed by the current authors. The progressive growth of the columnar dendrite trunks from the ingot surface into the centre, the nucleation and growth of the equiaxed crystals including the motion of the equiaxed crystals, the thermal and solutal buoyancy flow and its interactions with the growing crystals (equiaxed and columnar), the solute partitioning at the solid-liquid interface during solidification and the solute transport due to melt convection and equiaxed sedimentation, the columnar-to-equiaxed transition (CET) were considered. As modelling result the mixed columnar-equiaxed macrostructure and different macrosegregation patterns can be predicted. Application of the aforementioned model is mainly limited by two factors: one is the extreme computational expense; one is the lack of the reliable parameters being required by the model. In order to perform a calculation of industry ingot (up to hundreds tons) on the base of the current computer resources, compromise is often made between the model capability and the computational feasibility, i.e. some necessary model simplifications have to be made. In this article the on-going works to scale-up the current models for the industry applications are reported.

Keywords: steel, ingot casting, macrosegregation, multiphase simulation.

1. Introduction

Most valuable experimental researches on the macrosegregation in large steel ingots were done in ca. one century ago [1-2]. A series of steel ingots, scaled from a few hundred kilograms up to 172 tons, were poured and cut for segregation analysis. Primary knowledge was obtained, and typical segregation map in the large steel ingots was drawn [3-5], as shown in Figure 1. To date most segregation phenomena can be physically explained. Multiphase flow such as thermo-solutal convection, happening in the interdendritic and bulk regions, and crystal sedimentation during solidification is the key mechanism for the formation of segregation. The thermodynamics, solidification kinetics and thermal mechanics are also coupled with the flow phenomena, and contribute to the final segregation results.

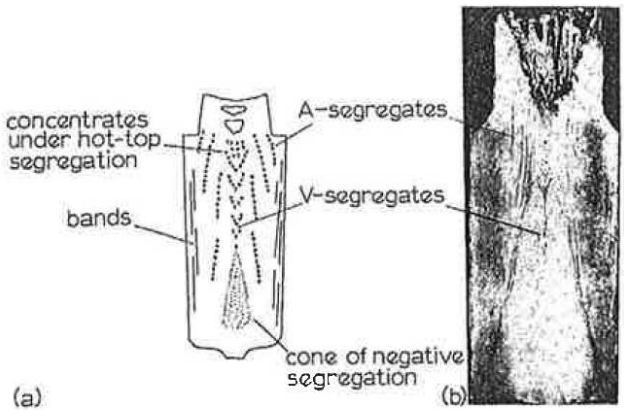

Figure 1. Typical segregation map in steel ingots (the figure is reproduced from [3]). (a) Schematic representation with '+' for positive and '-' for negative segregation; (b) sulphur print of a 10-ton ingot.

Today such experimental trials due to extremely high cost were only carried out occasionally with caution [6-9]. Instead mathematical (both analytical and numerical) modelling approach becomes a most efficient tool for this purpose. Some progresses were reviewed by other authors [9-12]. Understanding to the segregation mechanism was significantly improved by the mathematical models. Unfortunately, the picture of Figure 1 is still not quantitatively reproducible with sufficient details by numerical models of today. The great challenge arises from the multiphase nature of the solidification phenomenon. The solution of the segregation problem demands a precise description of the multiphase flow, which occurs and interacts with the solidifying microstructure (dendritic morphology) at different length scales. From the flow dynamic point of view, at least three (hydrodynamic) phases are involved in a typical ingot casting during solidification: two moving phases (liquid and equiaxed crystals) and one stationary phase (columnar dendrite trunks). In other words, a model being able to reproduce the patterns of Figure 1 needs at least to consider these three phases. However, the limitation of early computational hardware resource has prevented people from considering so many phases. Compromise has to be made between the model capability and the computational feasibility. For example, Gu and Beckermann used a mixture liquid-columnar solidification model [13] and Combeau et al. used a two-phase equiaxed solidification model [8] to simulate the segregation in steel ingots, and some successes were achieved.

This article is not going to give a comprehensive review of the topic of macrosegregation models, but focuses on the relevant activities being taken up by the current authors at the University of Leoben. On the base of

previous work of Beckermann's [11, 14-17], a series of multiphase solidification and macrosegregation models were proposed. These include a two-phase globular equiaxed solidification model [18-19], a two-phase monotectic solidification model [20-21], a three-phase mixed columnar-equiaxed solidification model [22-23], an equiaxed solidification model with dendritic morphology [24-25] and a five-phase mixed columnar-equiaxed solidification model with dendritic morphology [26-27]. As the computational expense increases correspondingly with the increasing number of phases, the modelling activities are divided in two directions. One is to further develop comprehensive models by including as many as necessary phases and physics to solve as much as possible segregation features on one hand. Application of this kind of models may still rely on future enhancement of the hardware resource. On the other hand we can base on the available hardware resource by using possibly-simple model to solve the principal segregation phenomena of the industry ingots. This article is going to report some modelling examples by using a three-phase mixed columnar-equiaxed model [22-23]. The applicability of this model to the industry ingots is investigated, and some merits and limitations are discussed.

2. Characterization of the model

To characterize the three-phase mixed columnar-equiaxed solidification model, a benchmark (ϕ 66 mm x 170 mm) of a steel ingot was simulated. Macrosegregation formation due to the combined thermosolutal convection, grain sedimentation, and sedimentation induced convection was modelled. Details about the settings for this benchmark refer to previous publications [22-23, 28]. Model assumptions are summarized as follows:

- Solidification starts with an initial concentration Fe-0.34 wt.%C and an initial temperature of 1785 K, mould filling is ignored;
- Three phases considered are: the melt, globular equiaxed crystals and columnar dendrite trunks;
- Morphologies are approximated by step-wise growing cylinders for columnar dendrite trunks and spheres for globular equiaxed crystals;
- Columnar trunks grow from side and bottom walls, and the columnar tip front is explicitly tracked;
- A three-parameter heterogeneous nucleation law is used for the nucleation of the equiaxed crystals [29]. No fragmentation and grain attachment are considered;
- Shrinkage flow is ignored. The buoyancy force for the thermosolutal convection and crystal sedimentation is accounted for by a Boussinesq approximation;
- The equiaxed crystals ahead of the columnar tip front can move freely, but they can be captured by the columnar trunks as the local columnar volume fraction is beyond 0.2;
- Hunt's blocking mechanism [30] is applied for predicting CET (columnar-to-equiaxed transition);
- Constant heat transfer coefficients and constant ambient temperatures are assumed [22].

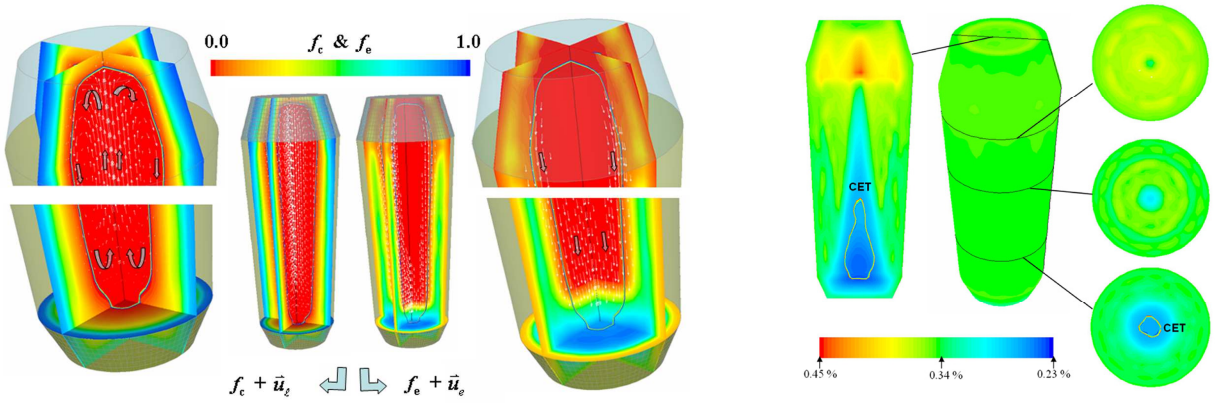

(a) (b)

Figure 2. a) Simulated solidification sequence (at 20 s) of the benchmark steel ingot. Volume fraction of the columnar and equiaxed phases, f_c and f_e, are shown in colour in two vertical and one horizontal sections, the velocity fields $\vec{u}_\ell$ and $\vec{u}_e$ are shown as vectors. The columnar tip front position is also marked. b) Predicted mix concentration c_{mix} in the steel ingot, scaled from 0.23 wt.% C to 0.45 wt.% C. The area of 100% equiaxed macrostructure is enveloped by the CET line. Here an arbitrary set of nucleation parameters ($n_{\max} = 5\times10^9\ \mathrm{m^{-3}}$, $\Delta T_\sigma = 2\ \mathrm{K}$, $\Delta T_N = 5\ \mathrm{K}$) is used to characterize the formation and sedimentation of equiaxed crystals and their impact on the macrosegregation.

The solidification sequence including sedimentation of the equiaxed crystals, the sedimentation-induced and thermosolutal buoyancy-induced melt convection are shown in Figure 2(a). The simulated solidification sequence agrees with the explanation of steel ingot solidification, as summarized by Campbell [31]. The columnar dendrites grow from the mould wall and the columnar tip front moves inwards. The equiaxed grains nucleate near the mould walls and in the bulk melt. The columnar dendrites are stationary, whereas the equiaxed grains sink and settle in the base region of the ingot. The accumulation of such grains at the base of the ingot has a characteristic cone-shape. The sedimentation of grains and the melt convection influence

the macroscopic solidification sequence and thus, the final phase distribution. More equiaxed grains will be found at the bottom and in the base region, while columnar structure will be predominant in the upper part of the ingot.

As the columnar tip front is explicitly tracked, the simulation shows that the columnar tip fronts from both sides tend to meet in the casting centre. However, in the lower part of the casting the accumulation of equiaxed grains stops the propagation of the columnar tip front. Its final position indicates the CET position. The CET separates the areas where only equiaxed grains appear from the areas where both columnar dendrites and equiaxed grains coexist.

The final macrosegregation distribution is predicted, as shown in Figure 2(b). From the simulation results it appears obvious that the main mechanism for the cone-shaped negative segregation in the base region is the grain sedimentation. The settling grains are poor in solute elements, thus their pile-up results in negative segregation in the bottom of the ingot. A further contributing factor to the strength of negative segregation arises from the flow divergence of the residual liquid through this zone at a late solidification stage. The positive segregation at the top region of the ingot is caused by the flow of the enriched melt in the bulk region. This kind of positive segregation coincides with classical experimental results [31]. It should be noted that channel segregations, which are frequently found in large steel ingots, are not predicted in such a benchmark ingot with reduced dimension.

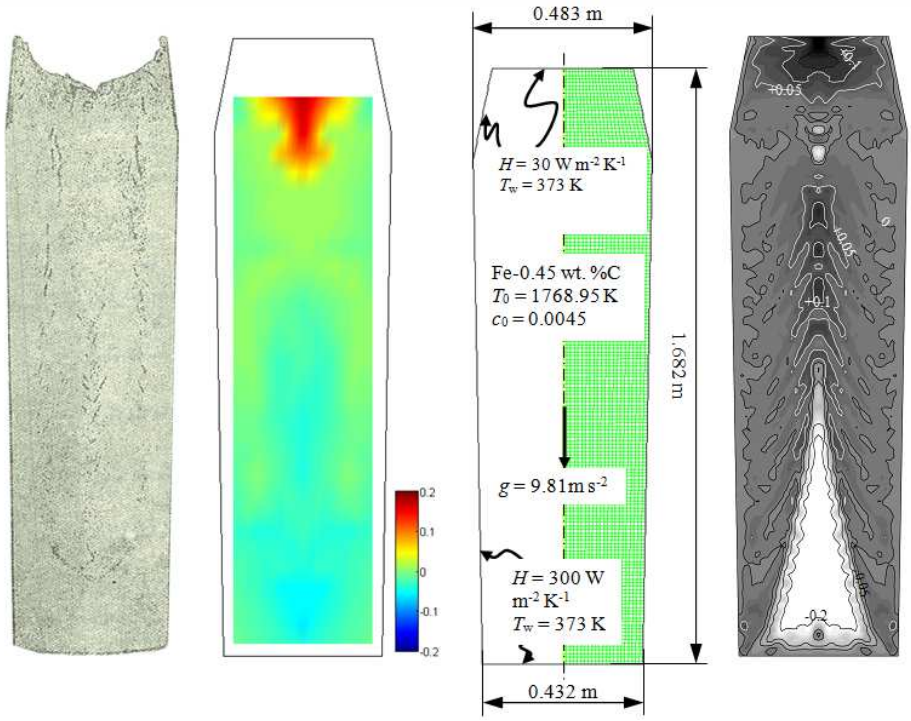

(a) surphur print (b) measured seg. (c) B.C. configuration (d) simulated seg.

Figure 3. Configuration of a 2.45-ton industry-scale steel ingot. (a)-(b) experiment [1], (c) simulation configuration and (d) simulated macrosegregation in grey scale (black for the positive segregation and light for the negative segregation) overlapped with isolines. The macrosegregation, both experimental (b) and simulated (d), is shown for the nominal mixture concentration $((c_{mix}\text{-}c_0)/c_0)$. Nucleation parameters: $n_{max} = 5\times10^9\ m^{-3}$, $\Delta T_\sigma = 2\ K$, $\Delta T_N = 5\ K$.

3. 2.45 ton ingot

The experimentally measured macrosegregation of a 2.45 ton big-end-up ingot (Fe-0.45 wt.%C) was reported [1]. The ingot had a section of square and was cast in a chilled mould. As reference, the segregation pattern in this ingot is numerically simulated and compared with the experiment, as shown in Figure 3. Due to lack of precise process description, some process parameters and boundary conditions have to be derived on the base of assumptions. The sulphur print of this ingot is shown in Figure 3(a). The measured mixture concentration $((c_{mix}\text{-}c_0)/c_0)$ map is shown in Figure 3(b). Configuration of this ingot, together with necessary boundary and initial conditions used for the calculation, is described in Figure 3 (c). More details about the simulation configurations are presented elsewhere [32], and the same three-phase model (Section 2.0) is used. 2D axis symmetrical simulations are performed to approximate the solidification behaviour in the square section ingot. The predicted solidification sequence is shown in Figure 4 and the segregation map is shown in Figure 3(d).

The global solidification sequence in this 2.45 ton ingot (Figure 4) is actually similar to what characterized by the previous small benchmark ingot (Figure 2). The sinking of the equiaxed crystals in front of the columnar dendrite tips leads to an accumulation of equiaxed

phase in the bottom region of the ingot. The accumulation of the equiaxed phase in the bottom region will block the growth of the columnar dendrite tips, i.e. CET occurs there, hence finally to cause a characteristic cone-shape distribution of equiaxed zone being enveloped in the CET line. Relatively strong negative segregation is predicted in the low-bottom equiaxed zone. With the sedimentation of large amount of equiaxed crystals downwards, the relatively-positive segregated melt is pushed upwards in the casting centre, hence to cause a positive segregation in the upper region. Despite the above similarity between the 2.45 ton ingot and the small benchmark ingot (Figure 2), significant differences are identified, which are described below.

Firstly, the flow is much more instable (Figure 4). The melt flow in the bulk region ahead of the columnar dendrite tip front is driven by three mechanisms: the solutal buoyancy which drives upwards; the thermal buoyancy which drives downwards; and the equiaxed sedimentation which drags the surrounding melt downwards. Generally the two downward driving forces are decisive, which cause the melt flows downwards along the columnar dendrite tip front. This downward flow along the columnar tips will push the melt to rise in the ingot centre. This rising melt will interact with the falling equiaxed crystals and with the downward flow near the columnar tip front, to form many local convection cells. The pattern of melt convection and crystal sedimentation becomes chaotic. These local convection cells are developed or suppressed dynamically, and the flow direction in the cells changes with time as well. The flow instability and the flow chaotic behaviour are dependent on the ingot size (ingot height). Therefore, to explain the influence of the ingot size on the macrosegregation demands the knowledge about the influence of the ingot size on the flow pattern.

Secondly, a streak-like segregation pattern (Figure 3(d)) in the mixed columnar-equiaxed region is predicted, which does not occur in the small ingot (Figure 2(b)). Concrete explanation to this segregation pattern demands more detailed analysis of the flow and sedimentation and their interaction with the solidification, nevertheless a tentative hypothesis is proposed as follows. As the equiaxed crystal can be captured (crystal entrapment) by the growing columnar trunks, the entrapment of the equiaxed crystals will lead to a heterogeneous, i.e. streak-like, phase distribution between the columnar and equiaxed immediately behind the columnar tip front, as seen in Figure 4(b)-(d). The resistance to the interdendritic flow by the columnar trunks and the entrapped equiaxed crystals are different, therefore the flow direction of the melt in this region is slightly diverted by the heterogeneous phase distribution. This diverted-flow can only be visible in the carefully zoomed view. As the macrosegregation is extremely sensitive to the interdendritic flow, it is not surprising that the induced macrosegregation (Figure 3(d)) takes the similar streak-like pattern of the phase distribution (Figure 4(d)).

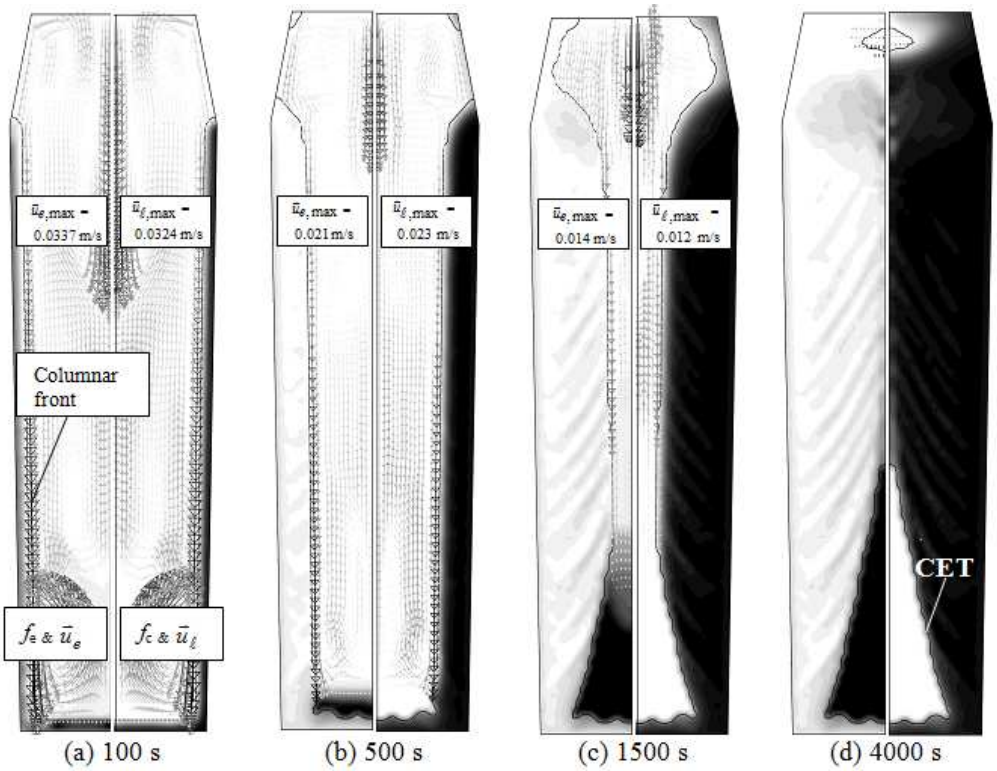

Figure 4. Solidification sequence of the 2.45 ton ingot. The volume fraction of each phase (f_e or f_c) is shown in gray scale from 0 (bright) to 1 (dark). The left half of each figure shows the evolution of equiaxed volume fraction (f_e) together with the equiaxed sedimentation velocity ($\vec{u}_e$) in black arrows. The right half of each figure shows the evolution of columnar volume fraction (f_c) together with the melt velocity ($\vec{u}_\ell$) in black arrows. The columnar dendrite tip position also marked with a black solid line.

One may notice that this streak-like segregation has a similar contour as the classical A-segregation, but it is still not clear if the classical A-segregation is the same one as steak-like segregation or originates from such streak-like segregation. According to the mostly-accepted empirical explanation, A-segregation belongs to a kind of channel segregation in large steel ingots, which originates and develops in the stationary dendritic mushy zone. A recent study of the authors [33-34] in a Sn-Pb laboratory casting has found that the channel segregation can originate and develop in a pure columnar solidification, where no equiaxed crystal exists. Therefore, we name the streak-like segregation here as a quasi-A-segregation. To form this quasi-A-segregation, the sedimentation of equiaxed crystals and its interaction with the columnar tip front and melt flow seem to play important role. Details about the formation mechanism for this kind of quasi-A-segregation are still to be verified.

Thirdly, the simulation of the 2.45 ton ingot shows an isolated hot spot in the upper part (Figure 4(d)), which takes much long time to solidify. As the middle part of the ingot is already blocked by the columnar trunks, the solidification of the hot spot behaves like a mini-ingot. Sedimentation of the equiaxed crystals in the mini-ingot will cause a small region of negative segregation, as shown in Figure 3(d). This kind phenomenon happens very often in long (small section) ingot casting or in the continuously-cast round billet casting, and it is called as 'bridging and mini-ingotism' [35]. The experimental result of Figure 3(b) seems to show that no such 'bridging and mini-ingotism' occurs, as no such negative segregation zone is identified. It implies that the heat transfer boundary conditions applied in the current simulation might not be coincident with the reality.

The segregation along the ingot centreline is analysed, and compared with the experiment, as shown in Figure 5. The experiment shows the negative segregation in the lower part and positive segregation in the upper part. The model also shows the same tendency. They agree with each other qualitatively. However, the negative segregation in the lower part is predicted more severe than the experimental result. The overestimation of the negative segregation in the lower part by the model may come from two aspects. One is the assumption of globular equiaxed morphology, which can cause significant overestimation of the sedimentation-induced negative segregation according to Combeau et al. [8]. The other aspect is the error assumption of the equiaxed nucleation parameters.

In order to demonstrate the role of the equiaxed phase in the formation of segregation, an additional calculation is performed by ignoring the occurrence of the equiaxed phase. This case seems to show better agreement with the experiment, especially in the middle and lower part (Figure 5). The experimental result falls actually in a range between the two calculations. Based on the above two simulations, one may anticipate that in the reality a certain amount of equiaxed crystals would appear during the solidification of such a 2.45 ton ingot, but the amount of equiaxed crystals is overestimated by the current nucleation parameters.

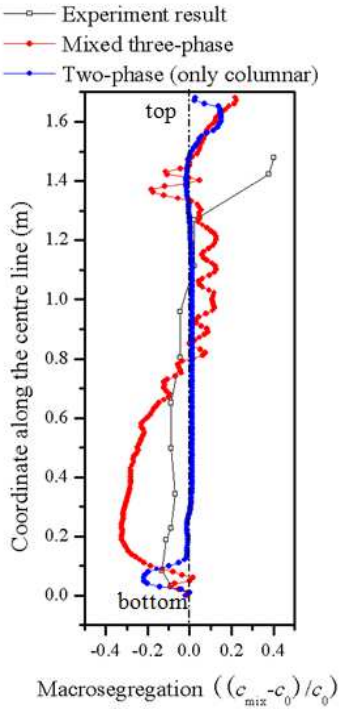

Figure 5. Comparison of the numerically predicted macrosegregation ($(c_{mix}-c_o)/c_o$) along the ingot centreline with the experiment [1]. Two simulations are performed: one is to consider the mixed columnar-equiaxed solidification ($n_{max}=5\times10^9\ m^{-3}$, $\Delta T_\sigma=2\ K$, $\Delta T_N=5\ K$); one is to ignore the appearance of equiaxed crystal.

The quantitative disagreement between the experiment and the calculations in top part of the ingot is mainly due to the formation of the cavity, which is not considered by the current model.

One should emphasize that the motivation of the current study is to validate the mixed columnar-equiaxed model, hence to explore the limitations of the model. We are not going to adjust the process parameters without evidence to cater for the experiment results. Since the experiments were made decades ago and many of the process parameters and material properties were not reported, the current simulation results can only reproduce the experiment results qualitatively.

4. 3.3 ton ingot

A forging ingot, 3.3 ton, was reported by Combeau and co-authors [8]. As a further step to validate the current three-phase solidification model, this ingot is also simulated. The shape of the ingot was actually octagonal, and an industry multicomponent alloy was poured, but here only a 2D axis symmetrical calculation for a simplified binary alloy (Fe-0.36 wt.%C) is performed. Process parameters and materials' data as reported in literature [8] are referred, but some unknown parameters have to be assumed for this preliminary calculation. Mould filling is ignored, and the nucleation parameters are assumed as: $n_{max}=2\times10^9\ m^{-3}$, $\Delta T_\sigma=2\ K$, $\Delta T_N=5\ K$. As

no sufficient information for the exothermal powder being added on the hot top is provided, it is here treated as a refractory material. Different from the aforementioned calculations for the small benchmark and 2.45-ton ingots, here the mould system is included in the calculation.

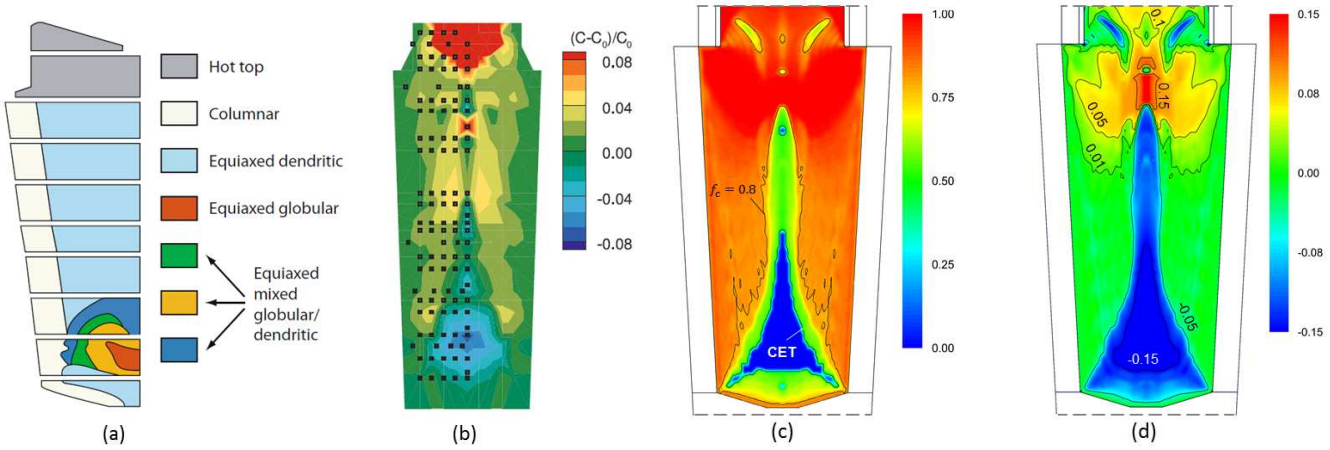

Figure 6. Modelling results of a 3.3-ton steel ingot: (a) experimentally measured macrostructure; (b) experimentally measured macrosegregation; (c) simulated macrostructure (volume fraction of columnar phase) and CET line; (d) simulated macrosegregation (colour scale overlapped with isolines). The macrosegregation, both experimental (b) and simulated (d), is shown for the nominal mixture concentration ($(c_{mix}\text{-}c_0)/c_0$). Nucleation parameters for the calculation are $n_{max} = 2\times10^9\ m^{-3}$, $\Delta T_\sigma = 2\,K$, $\Delta T_N = 5\,K$. The experimental results and casting configuration are reproduced from the literature [8].

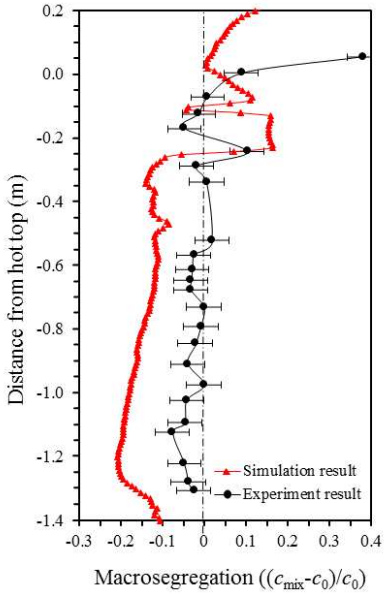

Figure 7. Comparison of the numerically predicted macrosegregation ($(c_{mix}\text{-}c_0)/c_0$) along the ingot centreline with the experiment [8].

The predicted macrostructure and macrosegregation are compared with the experimentally reported results, as shown in Figure 6 and Figure 7. Qualitatively, satisfactory agreement between them regarding to both macrostructure and macrosegregation is achieved. For example, the bottom equiaxed zone, accompanying relatively strong negative segregation (cone-shape), is predicted. This cone-shape negative segregation is mainly due to the equiaxed crystal sedimentation. Above the tail of the cone-shape negative segregation zone, there is a positive segregation zone (experimentally-shown only one point). Mechanism to form such positive segregation zone is due to the transport of the solute-enriched melt in the bulk. In the upper region of the ingot, just below the hot top, when the columnar dendrite tips, growing from side walls, meet together in the casting centre, some solute-enriched melt is 'frozen' there, to form this positive segregation. The late solidification of the hot top behaves as a mini-ingot. Sedimentation of the equiaxed crystals continues in the mini-ingot, but the crystals can only settle in the bottom of the mini-ingot, causing a small negative segregation zone in the bottom of the mini-ingot. Finally, a large positive segregation occurs in the hot top. Notice that the numerically predicted position of this positive segregation zone is much higher (Figure 7) and the predicted segregation is less severe than the experimental one.

Despite of the above agreement, the quantitative difference between numerically predicted and experimentally reported results is still significant. A cone-shape equiaxed zone with a long tail extending beyond the middle height of the ingot is predicted (Figure 6c), while the experimentally found equiaxed zone does not show a cone-shape, instead, the equiaxed zone is more accumulated in the bottom region (Figure 6a). Although the cone-shape equiaxed zone was found typical in many ingots [1-3, 31], but it was not reported experimentally in this ingot. One interesting phenomenon is that the numerically predicted bottom equiaxed zone (Figure 6c) has the same cone-shape as the negative segregation zone (Figure 6d), while the experimentally reported equiaxed zone (Figure 6a) does not show the same shape as the bottom negative segregation zone (Figure 6b). Explanation to this phenomenon demands further study. Another difference between the simulation and the experiment is the overestimation of the sedimenta-

tion induced negative segregation. The main reasons were discussed above: one is the ignorance of the crystal dendritic morphology, and one is the assumption of the crystal nucleation parameters. The error prediction of the position and severity of the positive segregation in the hot top is mainly due to the ignorance of the cavity formation and the unknown condition of the exothermal powder at the top.

For the calculation of this 3.3-ton ingot, 8627 volume elements are divided, and parallel calculation was performed on 8 cores (Intel Nehalem Cluster 2.93 GHz), and the simulation time was about 2 weeks.

5. Discussions

This article reported the on-going activities of the authors' group to scale-up a mixed columnar-equiaxed solidification model for the industry applications. Three examples were analysed to evaluate the potentials and limitations of the model.

5.1 Model potentials

Firstly, the simulated solidification sequence, the sedimentation of the equiaxed grains, the growth of the columnar tip front and the formation of the final macroscopic phase distribution fit with the widely accepted explanations of experimental findings, as summarized by Campbell [31]: "The fragments (equiaxed grains) fall at a rate somewhere between that of a stone and snow. They are likely to grow as they fall if they travel through the undercooled liquid just ahead of the growing columnar front, possibly by rolling or tumbling down this front. The heap of such grains at the base of the ingot has a characteristic cone shape." This kind of multiphase flow dynamics and interactions among the melt, equiaxed crystals and growing columnar trunks are the key phenomena for modelling the segregation pattern of Figure 1. They are considered by the current model.

Secondly, it is also verified by the above modelling examples that the most typical segregates, the concentrated positive segregation under hot-top and the cone of negative segregation at the base of the ingot, can be simulated by the model. A widely accepted explanation to the formation of the cone-shaped negative segregation is verified, again in Campbell's words: "The heap of equiaxed grains at the base of the ingot has a characteristic cone shape. Because it is composed of dendritic fragments, its average composition is that of rather pure iron, having less solute than the average for the ingot." A further contributing factor to the purity of the equiaxed cone region probably arises from the divergence of the flow of residual liquid through this zone at a late stage in solidification. The simulated negative segregation formation process by equiaxed crystal sedimentation (Figure 2 and 4) seems to have reproduced the experimental phenomenon. Mechanisms for positive segregations under the hot-top in steel ingots are diverse. It is generally agreed that they are caused by the melt convection in the bulk region or through the partially solidified and/or remelted mushy zone. For example, the upper positive segregation is explained by the melt convection in the bulk region, because the light solute-rich melt rises. Actually, according to the recent modelling results, with the sedimentation of large amount of equiaxed crystals downwards, the relatively-positive segregated melt is pushed upwards, instead of 'rise' by itself, in the casting centre, hence to cause a positive segregation zone in the upper region.

Thirdly, it has demonstrated the possibility to calculate the distribution of columnar and equiaxed structure. The upper region of the ingot mainly consists of columnar dendrites, whereas a larger amount of equiaxed grains are predicted in the bottom region. Within the CET enclosed region, only the equiaxed phase exists, while outside of the CET region both columnar and equiaxed phases coexist. The macrostructure strongly depends on some modelling and process parameters, i.e. the equiaxed nucleation parameters ΔT_N, $n_{\max}$, ΔT_σ, the primary columnar space λ_1, and boundary conditions.

Finally, the capability of the current model for the interdendritic-flow-induced channel segregation was also verified [33-34], but not precisely shown in the above examples. The modelling result for the channel segregation is extremely sensitive to the grid resolution. Grid size less than 0.1 mm is often required, and this is unrealistic for the large industry ingots on the base of the current computer resources. One interest finding by the current three-phase solidification model, worth mentioning here, is the streak-like (quasi-A) segregation pattern, which occurs due to the columnar-equiaxed interaction at the columnar tip front. The streak-like segregation pattern has some similarity to the classical A-segregation, but it is not clear if the classical A-segregation is the same one as or originates from the streak-like segregation. It is still to be verified.

5.2 Limitation of the model

Importance of the process conditions, e.g. the pouring temperature, pouring method, mould materials and interfacial heat transfer between the ingot and the mould, etc., is obvious for the quantitative accuracy of the simulated solidification process, hence of the macrosegregation. It is not discussed here. Following discussions focus on the aspect of numerical model.

Firstly, the influence of the nucleation event on the macrosegregation was addressed in the example of 2.45-ton ingot. The origin of the equiaxed grains may be due to different mechanisms, e.g. heterogeneous nucleation, and/or fragmentation and detachment of dendrites by re-melting, and/or nucleation formed during pouring by contact with the initial chilling of the mould. The recent model condenses all these phenomena into a single effective nucleation description. Here, a three-parameter heterogeneous nucleation law [29] is applied for the origin of equiaxed crystals. The reliable

nucleation parameters can be only possibly obtained experimentally.

Secondly, no shrinkage cavity and porosity is considered. This ignorance will influence the accuracy of the calculation, especially in the hot-top region. As shrinkage contributes or influences the interdendritic flow, it will influence the final distribution of the channel segregation as well. However, the global segregation pattern, e.g. the concentrated positive segregation in the upper region and the cone of negative segregation at the base of the ingot, will not be significantly influenced by the shrinkage.

Thirdly, no thermal mechanics is considered. The thermal mechanical shrinkage of the solidified outer shell of the ingot will influence the internal flow, but this may not be so significant. What is most important is the deformation of the growing crystals, due to the thermal shrinkage or the solid phase transition, which would have great impact on the flow near end of solidification at the centreline. The 'V' segregation is mostly related to such deformation. This 'V' segregation is not modelled by the current model.

Finally, the current three-phase model does not include dendritic morphology. This ignorance has overestimated the cone of the negative segregation at the base, as what we see in Figure 5 and 7. In order to consider the dendritic morphology, more phases, i.e. the interdendritic melt, must be separately considered. In the authors' group, a five-phase model was developed to consider the mixed columnar-equiaxed solidification with dendritic morphology [26-27]. The calculation expense is so heavy to prevent from applying it in the industry ingots. However, the validity of this model for such purpose has been verified, but in a laboratory Al-4.0 wt.%Cu ingot casting, as shown in Figure 8. A cylindrical casting (ϕ 75 mm x 133 mm) was poured, analysed for both macrostructure and macrosegregation. The experimental results were used to validate the numerical simulations. Satisfied agreement between them was obtained, as reported elsewhere [36-37].

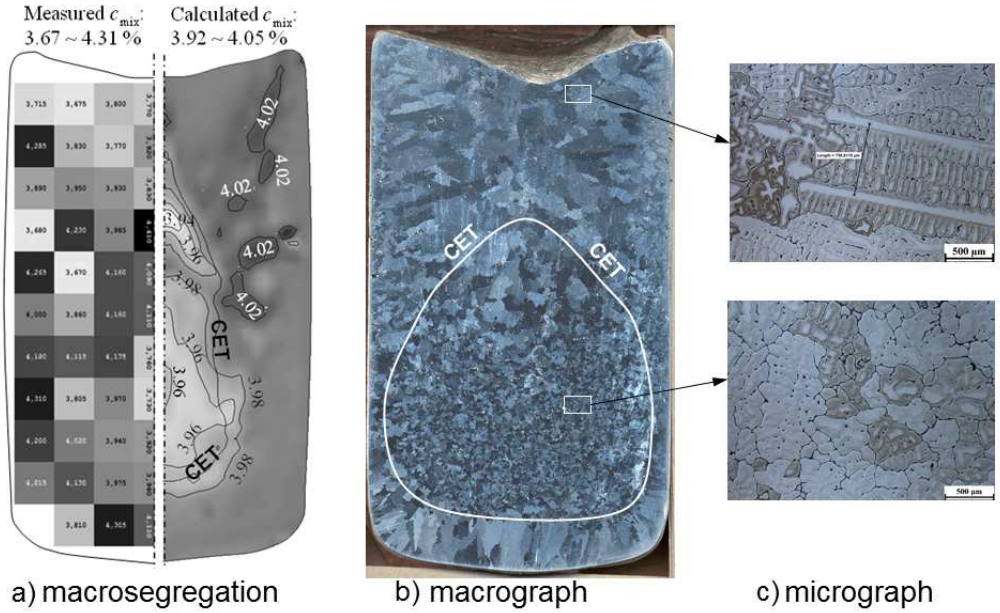

Figure 8: An example of the modelling result of an Al-4wt.%Cu ingot with a five-phase mixed columnar-equiaxed solidification model with dendritic morphology. (a) Comparison of the measured (spark analysis) macrosegregation (left half) with the calculated one (right half). The casting is poured at 800 °C. c_{mix} is shown in gray scale (dark for the highest and light for the lowest value). CET positions are plotted. This numerical simulation result shows satisfactory agreement to the as-cast macrostructure (b) macrograph, (c) micrograph.

5.3 Outlook

The future modelling activities for the macrosegregation in large steel ingots will keep in two directions. One is to further enhance the model capability by including more physics such as solidification shrinkage, thermal mechanics, dendrite fragmentation as new crystal origin, etc. Another direction is to further validate and improve the existing multiphase model, and to apply it for the purposes of solving engineering problem and enhancing fundamental understanding of different segregation phenomena.

1. Thanks to the work of the Iron Steel Institute [1], many steel ingots scaled from 600 kg to 172 tons were poured and sectioned for segregation analysis. This work provides most valuable information for the validation of the numerical models.
2. The existing model can be applied for the process parameter study. Despite of the difficulty to quantitatively reproduce the segregation pattern of the reali-

ty, the influence of the process parameters, such as casting geometry, mould materials, pouring temperature, or other engineering measures, on the segregation can be well described by the model. By performing such parameter study, metallurgists would achieve idea for the process optimization.

3. Any segregation mechanism, as proposed from the experimental observation, can (should) be verified quantitatively by the mathematical (numerical or analytical) model. The three-phase model can help to explain many well-known segregation phenomena in details. It may also help to explore the new segregation phenomena, which are caused by the multiphase flow. For example, the question of streak-like segregation, here we name it as a quasi-A-segregation, is first raised by the authors on the base of current modelling result. The equiaxed-columnar interaction at the columnar dendrite tip front and its influence on the melt flow seems to induce such kind of streak-like macrosegregation.

Acknowledgement

The authors acknowledge the financial support by the Austrian Federal Ministry of Economy, Family and Youth and the National Foundation for Research, Technology and Development.

References

[1] J. Iron Steel Institute, 103(1926), p. 39-176.
[2] Marburg E.: J. Met., 5(1953), p.157-172.
[3] Moore J.J., Shah N.A.: Int. Metals Rev., 28(1983), p. 338-356.
[4] Blank J.R., Pickering F.B.: The solidification of metals, London: The Iron & Steel inst., 1968, p. 370.
[5] Yamada H., Sakurai T., Takemonchi T., Suzuki K.:Proc. Annual Meeting of AIME, Dallas, 1982, A82-39, p.1-6.
[6] Klug J.S., Ernst C., Hartmann L.: Proc. SteelSIM, Düsseldorf, 27 June – 1 July 2011.
[7] Broytman O.A., Yu D., Monastyrsky A., Ivanov I.: Proc. SteelSIM, Düsseldorf, 27 June – 1 July 2011.
[8] Combeau H., Zaloznik M., Hans S., Richy P.E.: Metall. Mater. Trans., 40B(2009), p.289-304.
[9] Lesoult G.: Mater. Sci. Eng. A, 413-414 (2005), p. 19-29.
[10] Flemings M.C.: ISIJ Int., 40(2000), p. 833-841.
[11] Beckermann C.: Int. Mater. Rev.: 47(2002), p. 243.
[12] Ohnaka I.: ASM Handbook, 15 – Casting, ASM Int., USA, p.136.
[13] Gu J.P., Beckermann C.: Metall. Mater. Trans., 30A(1999), p. 1357.
[14] Ni J., Beckermann C.: Metall Mater Trans 22B(1991), p.49.
[15] Wang C.Y., Beckermann C.: Metall Trans 24A(1993), p. 2787.
[16] Beckermann C., Viskanta R.: Appl Mech Rev 46(1993), p.1.
[17] Wang C.Y., Beckermann C.: Metall Mater Trans 27A(1996), p.2754.
[18] Wu M., Ludwig A., Bührig-Polaczek A., Sahm P.: Int. J. Heat Mass Transfer, 46(2003), p. 2819.
[19] Ludwig A., Wu M.: Metall. Mater. Trans., 33A(2003), p.3673.
[20] Wu M.; Ludwig A., Ratke L.: Metall. Mater. Trans., 34A(2003), p.3009.
[21] Wu M.; Ludwig A., Ratke L.: Modell. Simu. Mat. Sci. Eng., 11(2003), p.755.
[22] Wu M.; Ludwig A.: Metall. Mater. Trans., 37A(2006), p.1613.
[23] Wu M.; Ludwig A.: Metall. Mater. Trans., 38A(2007), p. 1465.
[24] Wu M., Ludwig A.: Acta Mater., 57(2009), p. 5621.
[25] Wu M., Ludwig A.: Acta Mater., 57(2009), p. 5632.
[26] Wu M., Fjeld A., Ludwig A.: Comp. Mater. Sci.: 50(2010), p. 32.
[27] Wu M., Fjeld A., Ludwig A.: Comp. Mater. Sci.: 50(2010), p. 43.
[28] Wu M., Könözsy L., Ludwig A., Schützenhöfer W, Tanzer R.: Steel Res. Int., 79(2008), p.637.
[29] Rappaz M.: Int. Mater. Rev., 34(1989), p.93.
[30] Hunt J.D.: Mater. Sci. Eng., 65(1984), p. 75.
[31] Campbell J.: Castings, Butterworth Heinemann Ltd, Oxford, 1991.
[32] Li J., Wu M., Ludwig A.: Int. Conf. on MCWASP XIII, June 17-22, 2012, Austria.
[33] Li J., Wu M., Hao J., Ludwig A.: Comp. Mater. Sci., 55(2012), p.407.
[34] Li J., Wu M., Hao J., Kharicha A., Ludwig A.: Comp. Mater. Sci., 55(2012), p.419.
[35] Moore J.J.: Iron & Steel Soc., 3(1984), p.11-20.
[36] Wu M., Nunner G., Ludwig A., Li J.H., Schumacher P.: IOP Conf. Series: Mater. Sci. Eng., 27(2011), doi: 1088/1757-899X/27/1/012018.
[37] Wu M., Ahmadein M., Ludwig A., Kharicha A., Li J.H., Schumacher P.: Int. Conf. on MCWASP XIII, June 17-22, 2012, Austria.